

Hydrothermal Synthesis of Two Zinc Coordination Polymers with 1-(1H-Tetrazol-5-ylmethyl)-1H-benzotriazole Ligands

Su-Wen Sun,^[a] Lei Jin,^[a] Ping-Ping Shi,^[a] Ming-Liang Liu,^[a] Li-Hui Kong,^[a] and Qiong Ye*^[a]

Keywords: In situ synthesis; Tetrazole; Zinc; Hydrothermal condition; Crystal structure

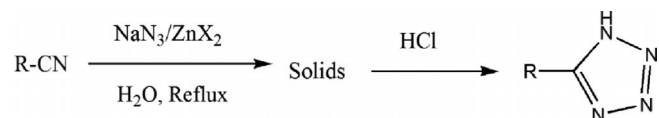
Abstract. The direct reaction of ZnBr₂ with H-1-mbtz [1-mbtz = 1-(1H-tetrazol-5-ylmethyl)-1H-benzotriazole] gives the two-dimensional complex [Zn(Br)(1-mbtz)] (**1**), whereas the reaction of benzotriazol-1-yl-acetonitrile with NaN₃ in the presence of water and a Lewis acid (ZnBr₂) affords the 2D coordination polymer [Zn₂(OH)(1-mbtz)₃H₂O] (**2**). The central zinc atom in **1** is bonded to one terminal bromine atom and three different nitrogen atoms from two tetrazole ligands and one BTA group (BTA = benzotriazole), and each 1-mbtz ligand is coordi-

nated to three zinc atoms forming a 2D framework. The coordination polyhedron around the metal atom in **2** is a slightly distorted trigonal bipyramid made up by one zinc atom, four nitrogen atoms as well as one oxygen atom, two of the 1-mbtz ligands coordinated to three zinc atoms and the third 1-mbtz ligand acts in a bidentate fashion, which leads to the formation of a complicated 2D network. The syntheses and solid-state structures of the two coordination polymers are reported.

Introduction

In recent years, the design of metal-organic frameworks (MOFs) containing central metal atoms and multi-functional ligands have triggered tremendous interests and attention owing to their fascinating structural diversities^[1–6] and potential applications in numerous fields such as catalysis, nonlinear optics, electrical conductivity, gas storage, magnetism, fluorescence, and ferroelectricity.^[7–12] In order to acquire designed frameworks and predictable properties, a wide range of research and studies are being focused on constructing novel MOFs by selecting versatile organic ligands and functional metal ions. Accordingly, heterocyclic carboxylic acids such as benzotriazolyl-, tetrazolyl-, pyridine-, and pyrazole- as building blocks have attracted much attention.^[13–20] Among these heterocyclic rings, especially, ligands based on tetrazolate have been one of the most attractive themes because they possess multiple coordination modes and have the ability to produce various types of MOFs that display abundant marvelous architectures.^[21–29] In 2001, Sharpless and co-workers described a safe, convenient and environmentally friendly approach for the synthesis of 5-substituted 1H-tetrazoles, which can be accomplished with water as solvent and zinc salts as catalysts.^[30,31] Ever since, there have been tremendous research interests aimed at investigation of in situ tetrazole ligand syn-

thesis through [2+3] cycloaddition reactions between organic cyano compounds and NaN₃ in the presence of Zn²⁺ ions as Lewis acid catalyst (Scheme 1). Hydrothermal or solvothermal syntheses acting as powerful methods to construct novel coordination polymers have been extensively developed. Xiong and co-workers^[32,33] have found that single crystals of coordination polymers can often be produced under hydrothermal conditions. As a result, combining the in situ tetrazole ligands syntheses and the utilization of hydrothermal techniques, a number of novel coordination polymers have been reported.^[34–36] In comparison with the direct tetrazole-synthesis method using tetrazole precursor derivatives (usually a cyano group), the in situ hydrothermal synthesis was shown to initiate [2+3] cycloaddition of azides with nitriles and has absolute advantages. Firstly, the benefit of the in situ method is making all the reactions occur just in one step, being able to assemble the desired product in one step, whereas the direct method maybe require more than one step. Secondly, the in situ method is highly efficient as there is no need for ligand synthesis and thus being environmental friendly.^[37] Lastly, it is easier to get more complicated structures through the in situ method.



Scheme 1.

Herein we have repeated the Demko-Sharpless reaction under hydrothermal conditions in an effort to generate crystals that may follow the structural regular patterns of the solid intermediates. Therefore, we report the syntheses and crystal

* Dr. Q. Ye
Fax: +86-25-52090626
E-Mail: yeqiong@seu.edu.cn

[a] Ordered Matter Science Research Center
College of Chemistry and Chemical Engineering
Southeast University
Nanjing 211189, P. R. China

Supporting information for this article is available on the WWW under <http://dx.doi.org/10.1002/zaac.201300206> or from the author.

structures of two 2D zinc tetrazole coordination polymers, where BTA (BTA = benzotriazole) and tetrazole ligands exist together. The direct reaction of ZnBr_2 with H-1-mbtz under hydrothermal reaction conditions was completed. Surprisingly, the reaction products obtained in the in situ synthesis and the direct synthesis have quite different framework structures.

Results and Discussion

$[\text{ZnBr}(1\text{-mbtz})]$ (**1**) is obtained by the treatment of H-1-mbtz, ZnBr_2 , and H_2O under hydrothermal conditions, whereas the reaction of benzotriazol-1-yl-acetonitrile with NaN_3 in the presence of water and a Lewis acid (ZnBr_2) under similar conditions yields $[\text{Zn}_2(\text{OH})(1\text{-mbtz})_3\text{H}_2\text{O}]$ (**2**). For each reaction the IR spectrum indicates the absence of the cyano group, which is consistent with [2+3] cycloaddition between the cyano group and the azide anion, suggesting that cyano has changed to the tetrazole with several typical tetrazolyl group peaks at 1453, 1475, and 1343 cm^{-1} . Bands at 1555, 1483, 1155, 789, and 705 cm^{-1} are attributed to the benzotriazole aromatic ring. Disappearance of the N–H vibrations of the ligand suggests that the nitrogen atoms of the tetrazole ligand were ionized to balance the charge of the metal ion. In the IR spectrum of **2**, strong peaks and wide band over 3400 cm^{-1} suggests that the hydroxyl group and coordinated water molecules are present.

Compound **1** crystallizes in the monoclinic system, space group $P2_1/c$. Crystallographic data of **1** (Table 1) reveals that

Table 1. Crystal and refinement data of **1** and **2**.

	1	2
Empirical formula	$\text{C}_8\text{H}_6\text{BrN}_7\text{Zn}$	$\text{C}_{48}\text{H}_{40}\text{N}_{42}\text{O}_3\text{Zn}_4$
Formula weight	345.48	1514.70
Temperature /K	293(2)	293(2)
Radiation, Wavelength /Å	Mo- K_α ; 0.71073	Mo- K_α ; 0.71073
Crystal system	monoclinic	triclinic
Space group	$P2_1/c$	$P\bar{1}$
Unit cell parameters		
a /Å	7.3032(14)	8.4270(17)
b /Å	8.521(2)	9.5626(19)
c /Å	17.015(3)	18.648(4)
α /°	90	80.83(3)
β /°	93.194(11)	79.79(3)
γ /°	90	73.56(3)
Volume /Å ³ , Z	1057.2(4), 4	1408.9(5), 1
Calculated density /g·cm ⁻³	2.171	1.785
Crystal size /mm ³	$0.2 \times 0.2 \times 0.2$	$0.2 \times 0.2 \times 0.2$
θ Range for data collection /°	3.39–27.47	3.14–27.48
Color	colorless	colorless
Crystal shape	block	block
Reflections collected	10210	14497
Independent reflections	2398 [$R_{\text{int}} = 0.0523$]	6401 [$R_{\text{int}} = 0.1286$]
Parameters refined	154	442
Goodness-of-fit on F^2	1.042	1.039
Final R indices [$I > 2\sigma(I)$]	$R_1 = 0.0340$, $wR_2 = 0.0762$	$R_1 = 0.0852$, $wR_2 = 0.1630$
R indices (all data)	$R_1 = 0.0387$, $wR_2 = 0.0791$	$R_1 = 0.1422$, $wR_2 = 0.1814$
Largest diff. peak and hole /e ⁻ Å ⁻³	0.494 and -0.879	1.537 and -1.123

compound **1** adopts a two-dimensional coordination network and the asymmetric unit contains one 1-mbtz ligand and one zinc atom as well as one bromine atom. The local coordination environment around the central zinc ions can be best described as a slightly distorted tetrahedral arrangement (Figure 1), where each zinc ion is bonded to one terminal bromine atom (Br1) and three different nitrogen atoms [N1^i , N4^{ii} , N6; symmetry code: (i) $-x, 2-y, 2-z$; (ii) $x, 1.5-y, 0.5+z$], which belong to the tetrazole ligand (N1^i , N4^{ii}) and the BTA group (N6). The bond lengths of Zn–N range narrowly from 2.014(2) to 2.024(2) Å and the bond length of Zn1–Br1 is 2.3286 Å, showing the weaker binding force with the zinc ion. The Zn–N bond lengths are slightly shorter than those in $\text{Zn}(\text{OH})(3\text{-ptz})$ (3-ptz = 3-pyridyltetrazole) [2.042(4)–2.464(4) Å] and $\text{ZnCl}(4\text{-ptz})$ (4-ptz = 4-pyridyltetrazole) [2.026(4), 2.031(3), and 2.036(4) Å].^[38] Meanwhile, the N–Zn–N angles range from $103.75(10)^\circ$ to $114.22(1)^\circ$ and the N–Zn–Br angles from $108.07(7)^\circ$ to $114.72(7)^\circ$, which obviously have a large deviation from the ideal angle (109.47°) and thus creating distorted tetrahedra. Besides, each 1-mbtz ligand is coordinated to three central zinc atoms leading to the formation of the 2D layered network. As shown in Figure 2, two zinc atoms link the two 1-mbtz ligands resulting in the formation of a 16-

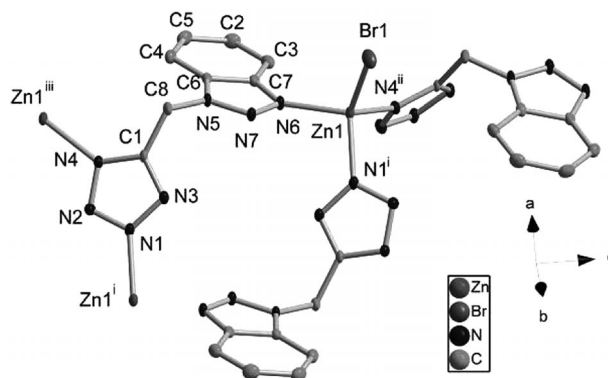


Figure 1. Coordination environments of the central Zn^{II} atoms in compound **1** (30% probability thermal ellipsoids). Hydrogen atoms are omitted for clarity. The label (i), (ii), and (iii) were generated by symmetry code: (i) $-x, 2-y, 2-z$; (ii) $x, 1.5-y, 0.5+z$; (iii) $x, 1.5-y, -0.5+z$; respectively.

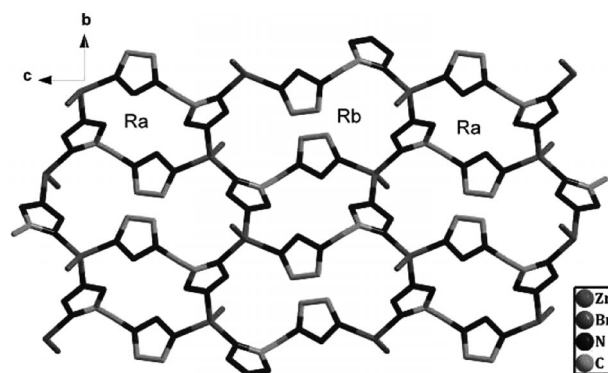


Figure 2. 2D sheet structure of compound **1** paralleled to bc plane. Hydrogen atoms and some ligands are omitted for clarity.

membered ring (Ra) composed of two zinc atoms, ten nitrogen atoms, and four carbon atoms ($\text{Zn}_2\text{N}_{10}\text{C}_4$), causing the BTA ring and tetrazole ring to have a dihedral angle of $65.635(8)^\circ$. The planes that the two BTA ligands occupy are nearly parallel with the dihedral angle of $0.00(8)^\circ$. Notably, the coordination bases are N1 atoms from tetrazole rings and N6 atoms from BTA rings. When the N4 atoms from tetrazole rings are included, another much larger ring (Rb) is formed, which is constructed by two BTA groups, four tetrazoles rings as well as four zinc ions (Figure 2). The two kinds of rings are adjacent and extend to the 2D network in RaRbRaRb sequence. Furthermore, the two BTA ligands in the Rb ring are nearly parallel too, with the dihedral angle of $0.00(9)^\circ$ and the distance of 3.4986 \AA . Viewed along the *a* axis, the neighboring two kinds of rings extend infinitely to outspread layers leading to the formation of the 2D plane (Figure 2). To get better insight into the intricate framework structure of **1**, its topological analysis was carried out. As discussed above, each central zinc atom links three nitrogen atoms and one vertex bromine atom, and thus can be defined as 4-connecting node, and the 1-mbtz ligand coordinated with three zinc atoms can be defined as a 3-connector, according to the simplification principle of the TOPOS software.^[39,40] The overall network topology of **1** can be described as an unprecedented (4,3)-connected framework (Figure 3) with Schläfli symbol of $\{3.12^2\}\{3.6.7\}2\{6.12^2\}$.

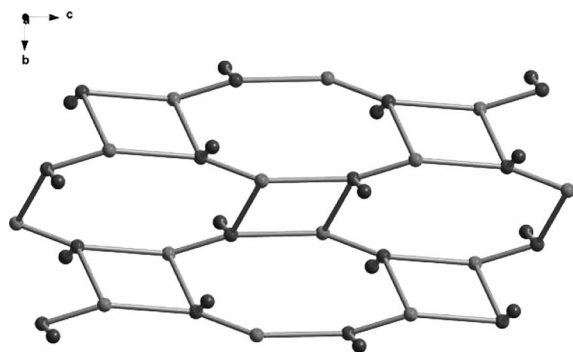


Figure 3. Topological representation of the 2D framework for **1**.

More interestingly, in the *ab* plane, the complicated two-dimensional polymer structure of compound **1** looks like a zigzag chain (Figure 4). The tetrazole ligand acts as μ_2 -tetrazolyl mode with two nitrogen atoms (1,3 position) bridging two zinc atoms to form a zigzag chain, owing to the nearly parallel arrangement of the BTA ligands on both sides of the chain. There are some weak non-classical hydrogen bonds (Table 3) found in the structure. Intermolecular $\text{C5-H5A} \cdots \text{N3}$ ($x, -1+y, z$) hydrogen bonds between the BTA ring and the tetrazole ring and $\text{C8-H8A} \cdots \text{Br1}$ ($x, 3/2-y, -1/2+z$) hydrogen bonds play a very important role in the stability of the two-dimensional network. Relatively short contacts $\text{C8-Br1} = 3.493 \text{ \AA}$ and $\text{C1-Br1} = 3.297 \text{ \AA}$ between the adjacent 2D supramolecular planes together with other noncovalent interaction-static attractive forces, like Coulomb and van der Waals forces, link the 2D network packing together by AAA sequence type along the *a* axis to a 3D framework.

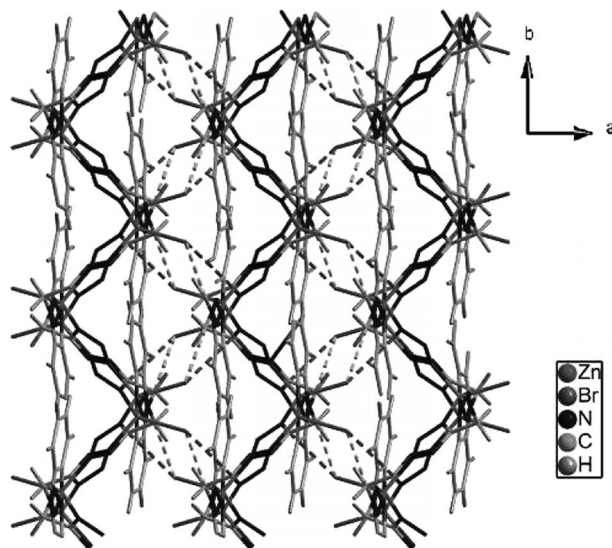


Figure 4. View of the extended zigzag-shape 3D supramolecular network in **1** along the *c* axis. The dashed line represents the C–Br short contact interactions.

Quite different from that found in compound **1**, the 2D structure of **2** is much more complicated, which was revealed by X-ray single-crystal diffraction investigation. Crystallographic data of **2** (Table 1) indicates that **2** is triclinic, space group $P\bar{1}$. The asymmetric unit contains two zinc atoms, three 1-mbtz ligands, one hydroxyl group as well as a water molecule, where the occupancy of the water molecule is one half. The BTA groups and tetrazole ligands have dihedral angles of $47.76(2)^\circ$, $68.85(3)^\circ$, and $82.71(2)^\circ$ respectively. There are two crystallographically independent central zinc atoms. The Zn1 atom is coordinated by four nitrogen atoms (N19, N12, N8^{iv}, N1^v; symmetry code: (iv) $1+x, -1+y, z$; (v) $3-x, 1-y, -z$), in which the N19 atom is from the BTA ligand and the others from the tetrazole group, and one oxygen atom O1. The Zn2 ion has a same coordination environment as the Zn1 ion, each Zn2 atom is bonded to four nitrogen atoms (N18, N15, N4^{vi}, N6^{viii}; symmetry code: (vi) $-1+x, 1+y, z$; (viii) $x, -1+y, z$) and one oxygen atom O1, which means the O1 is a bridge linking the two different central zinc atoms. Besides, the two zinc atoms are also linked by the C10–N15 tetrazole ligand. Uncommonly, the zinc atoms are pentacoordinate instead of quadridentate or hexadentate, as shown in Figure 5. The coordination polyhedron of the metal atom is a slightly distorted trigonal bipyramid performed through one zinc atom in a center, two nitrogen atoms (N8, N19 for Zn1; N6, N18 for Zn2) and one O1 atom in the equatorial plane with the deviation of the plane 1 and 2 being 0.1171 \AA and 0.2137 \AA and two nitrogen atoms (N1, N12 for Zn1; N4, N15 for Zn2) in the axis plane with the N1–Zn1–N12 equaling to $162.7(3)^\circ$ and the N4–Zn2–N15 equaling to $173.4(3)^\circ$. It is interesting to note that the adjacent two zinc ions (Zn1 and Zn2) together with the bridged O1 atom and one tetrazole ring result in a formation of a five-membered ring (R1) composed of two zinc atoms and two nitrogen atoms as well as one oxygen atom ($\text{Zn}_2\text{N}_2\text{O}$). Two R1 rings are separated by two

tetrazole rings and thus causing another plane (Zn1O1Zn2N4N2N1Zn1O1Zn2N4N2N1) (R2) with the mean deviation being 0.4028 Å. Furthermore, the bonds Zn1–N19 and Zn2–N18, which are from the two BTA parts, are approximately perpendicular to the plane of this large ring with dihedral angles between the BTA ring and the R2 being 83.27(1)° and 78.27(1)°, separately. All the Zn–N [2.176(7) Å, 2.062(7) Å, and 2.072(6) Å as well as 2.273(7) Å in the Zn1 atom, and 2.082(6) Å, 2.180(7) Å, and 2.091(7) Å as well as 2.197(7) Å in the Zn2 atom] bond lengths are normal, it is worth noting that the bond lengths of Zn–N are much longer than those found in compound **1**. The angles in the equatorial plane around each zinc atom range from 109.4(3)° to 139.6(2)° for Zn1 and 107.7(3)° to 126.7(3)° for Zn2, whereas the angles between axis atoms and the equatorial atoms for Zn1 being from 81.1(2)° to 100.5(3)° and for Zn2 range from 85.7(2)° to 93.3(2)°, which significantly deviate from those expected for an ideal trigonal bipyramid. The difference of the Zn–N bond lengths and the direction of the 1-mbtz ligands around each zinc atom must be primary factor to result in the formation of two different central zinc atoms.

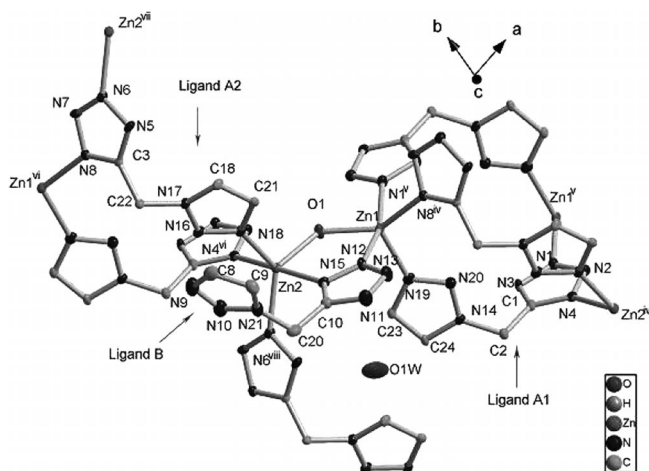


Figure 5. Coordination environments of the central zinc atoms in compound **2** (30% probability thermal ellipsoids). Hydrogen atoms and benzene rings are omitted for clarity. The labels iv, v, vi, vii, and viii were generated by symmetry code: (iv) $1+x, -1+y, z$; (v) $3-x, 1-y, -z$; (vi) $-1+x, 1+y, z$; (vii) $x, 1+y, z$; (viii) $x, -1+y, z$; respectively.

Similarly to compound **1**, each Zn1 ion shares two 1-mbtz ligands with adjacent Zn1 ion to create a 16-membered ring (R3) composed of two 1-mbtz ligands linked by two Zn1 atoms, in which the two benzotriazole rings are approximately parallel. The Zn1 ion also shares two 1-mbtz ligands with adjacent Zn2 and form a different 14-membered ring (R4) around Zn2 (Zn2N4C1C2N14N20N19Zn1N8C3C22N17N16N18), which is nearly vertical with the above 16-membered ring, the dihedral angle of the two rings equals to 85.860(8)°. In **2**, evidently, 1-mbtz ligands have two coordination patterns: ligand A1, the C2–N14 1-mbtz ligand, and ligand A2, the C22–N17 1-mbtz ligand, are tridentate coordinating to neighboring zinc atoms (two Zn1 and one Zn2 atoms, one Zn1 and two Zn2 atoms, respectively), through 1 and 3 positions (N1, N4 and N6, N8, respectively) of the tetrazole ring and the nitrogen

atoms (N19 and N18) of the BTA groups. Ligand B, the C20–N21 1-mbtz ligand, due to the particularity of N9 atom failed to coordinate, acts as in a bidentate fashion and coordinates to two zinc atoms (one Zn1 and one Zn2 atoms) leading to the formation of the complicated 2D network (Figure 6). The C3–N6 tetrazole ligand acts as a μ_2 -tetrazolyl mode through N6, N8 atoms (1,3 position) bridging Zn1 and Zn2 atoms, likewise, the C1–N3 tetrazole ligand adopts the μ_2 -tetrazolyl mode through N1, N4 atoms (1,3 position), however the C10–N15 tetrazole ligand adopts another kind of μ_2 -tetrazolyl mode (1,2 position).

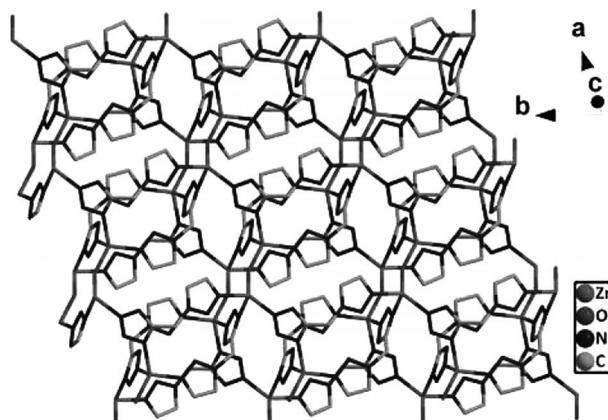


Figure 6. 2D sheet structure of compound **2**. Hydrogen atoms and benzene rings are omitted for clarity.

Moreover, each zinc atom is connected with four 1-mbtz ligands and one oxygen atom. There are many interesting hydrogen bonds, including C13–H13A...N5, C15–H15A...N12 weak intramolecular hydrogen bonds and C2–H2A...N7 ($1+x, -2+y, z$), C19–H19A...N3 ($2-x, 1-y, -z$), C20–H20A...N5 ($x, -1+y, z$), and C22–H22B...N20 ($-1+x, 1+y, z$) weak intermolecular hydrogen bonds (Table 3), and there are also some C–H... π interactions (Figure 7), which is evidence for an edge-to-face C–H... π interactions between the C(14) hydrogen atom of the BTA rings in one sheet to N(14) tetrazole rings in the next [C14...Cg1 distance: 3.499(0) Å, C14–H14A...Cg1 angle: 160.01(5)°] (Cg1 is the centroid of the tetrazole ring), and π – π stacking interactions (Figure 7) found in the 2D network. It needs to note that this π – π stacking interaction between the neighboring BTA rings is a novel three-layer interaction, where the middle ring shows the different orientation from those of the up and low layers, thus forming a interesting sand-

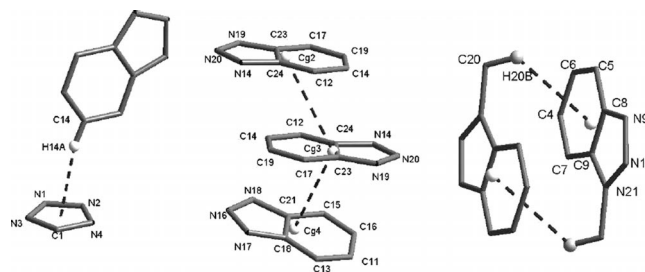


Figure 7. Three kinds of C–H... π and π – π stacking interactions in the compound **2**.

wich structure with the distance of Cg2–Cg3 and Cg3–Cg4 3.826(1) and 3.940(1) Å, respectively. These hydrogen bonds together with the C–H $\cdots\pi$ and π – π interactions obviously have a crucial impact on the stability of the arrangement of the 2D architecture. The organic ligands link inorganic zinc nodes to form 2D net sheets seeing along the *c* axis (Figure 6). Besides, seeing from the *a* axis we can discover these 2D networks have their thickness shown in Figure 8, which displays those rings clearly mentioned above.

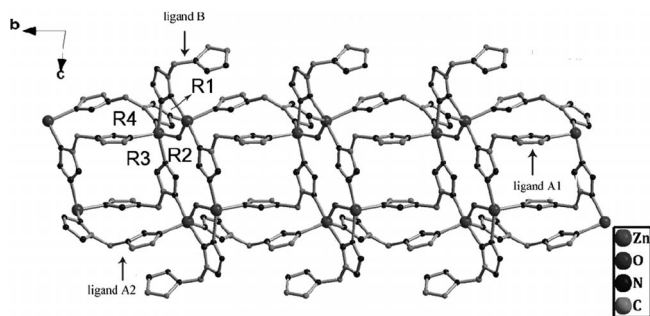


Figure 8. View of the thickness of the 2D network in compound **2** along the *a* axis. Hydrogen atoms and benzene rings are omitted for clarity.

From a topological perspective view, each central Zn1 and Zn2 atom may be considered as a five-connecting node and each O1 bridges to two zinc atoms and it is connection but not node. 1-mbtz ligands have two coordination patterns mentioned above, each ligand A1 and ligand A2 link to three central metal atoms and may be defined as three-connecting node, however, since each ligand B is only coordinated to two zinc atoms and it is only considered as connection and not node. Consequently, this results in the formation of 2D net with Schläfli symbol of $\{3.11^2\}\{3.6.7\}4\{3.6^2\}\{6.8.11^4\}\{6^2.8.9.11^2\}$ (Figure 9).

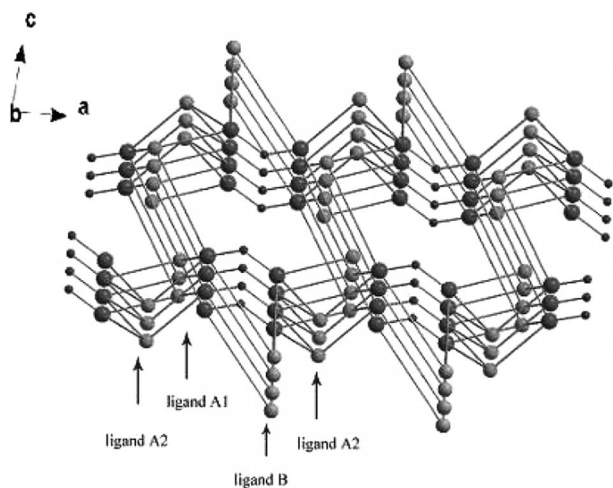


Figure 9. Topological representation of the 2D framework for compound **2**.

Among these 2D networks in **2**, another kind of C–H $\cdots\pi$ interaction is found, which is from the C20 hydrogen atom from the BTA ring to the adjacent BTA ring [C20 \cdots Cg5 dis-

tance 3.3027 (1) Å, C20–H20B \cdots Cg5 angle 106.529(6) $^\circ$] and forming two kinds of parallel interactions with the two BTA rings nearly paralleling, and the dihedral angle is 0.00(3) $^\circ$. There are also some free water molecules found and they connect the 2D network with intermolecular hydrogen bonds C20–H20B \cdots O1W and O1W–H1WA \cdots N11 ($2-x$, $1-y$, $1-z$), which also have acted as the bridges between adjacent 2D network and together with the above C20–H20B $\cdots\pi$ interactions to create a 3D network (Figure 10). The presence of water as spacers between the inorganic anions can alter the distances between the chains or layers and can also have distinctive hydrogen-bonding features, which influence the structural packing. Figure 10 shows the packing view of compound **2**, all of these approximate planes are packed together by AAA type along the *c* axis to a dense 3D framework.

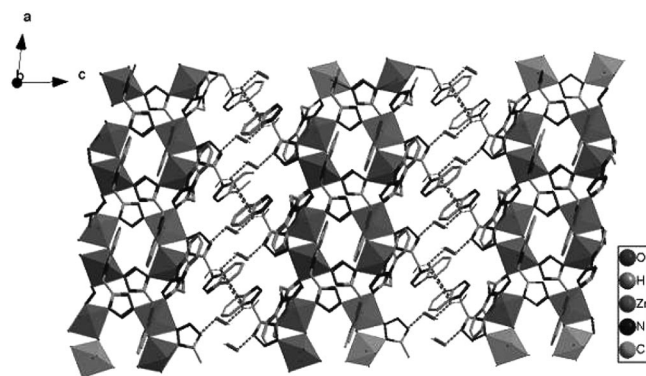


Figure 10. View of 3D framework structure of compound **2** in the *ac* plane. Some parts of the 2D network are omitted for clarity. The dashed line represents the CH–O, OH–N, and C–H $\cdots\pi$ interactions.

Similarly, we found that Xue^[34] has also conducted hydrothermal reactions through the two different methods and obtained different compounds, based on the 5-(4-pyridyl)tetrazolate ligand, which is consistent with our experiment. In our group such compounds synthesized through in situ hydrothermal methods and based on H-1-mbtz ligands have been reported before, for instance the C₃₂H₂₄Mn₅N₃₈O₄ compound,^[29] which is a 3D coordination polymer, and the arrangement around the three crystallographically independent metal atoms is different, except the H-1-mbtz ligands, this novel Mn^{II} coordination polymer is also formed by bridging azide anions and carboxylate ligands. As a result, this polymer is much complicated than the titled compound **2** in this paper.

Mixed inorganic-organic hybrid coordination polymers were investigated for fluorescence properties and they may have potential applications as fluorescence-emitted materials. The solid state fluorescent emission spectrum of complex **1** at room temperature shows that a maximum emission peak occurs at ca. 404 nm (excitation at 347 nm) (Figure S3). The photoluminescent mechanism may be considered to ligand-to-ligand transitions, which is in reasonable agreement with other zinc coordination polymers previously reported.^[42]

Conclusions

Two zinc tetrazole complexes were synthesized under hydrothermal conditions. Although they both display 2D planes, the local coordination arrangements around zinc atoms are different and form different rings, which assemble into two novel 2D structures. The structure of compound **2** obtained by in situ hydrothermal synthesis is much more complicated. Both complexes have rich hydrogen bonds, C–H $\cdots\pi$, and π – π interactions, which have great impact on the stability of the 2D network. The fluorescence property of **1** was studied, the results showed that a maximum emission peak occurred at ca. 404 nm.

Experimental Section

X-ray Diffraction Studies: Data collection of **1** and **2** were performed with Mo- K_{α} radiation ($\lambda = 0.71073 \text{ \AA}$) with a Rigaku SCXmini diffractometer by the ω scan technique at room temperature. The structure was solved by direct methods and refined with full-matrix least-squares technique using SHELXTL-97 software package.^[41] All non-hydrogen atoms were refined with anisotropic thermal parameters. Hydrogen atoms were placed in calculated positions (C–H = 0.96 \AA for Csp²), assigned fixed U_{iso} values [$U_{\text{iso}} = 1.2U_{\text{eq}}$ (Csp²/N) and $1.5U_{\text{eq}}$ (Csp³)] and allowed to ride. The crystal data and details concerning data collection and structure refinement are given in Table 1. Selected bond lengths and angles are listed in Table 2 and the hydrogen bonds are characterized in Table 3.

Table 2. Selected bond lengths / \AA and angles / $^{\circ}$ for compounds **1** and **2**.

1			
Zn1–N4 ⁱⁱ	2.014(2)	N4 ⁱⁱ –Zn1–N6	114.22(10)
Zn1–N6	2.021(2)	N4 ⁱⁱ –Zn1–N1 ⁱ	103.75(10)
Zn1–N1§3	2.024(2)	N6–Zn1–N1 ⁱ	104.07(10)
Zn1–Br1	2.3286(6)	N4 ⁱⁱ –Zn1–Br1	111.88(7)
		N6–Zn1–Br1	108.07(7)
		N1 ⁱ –Zn1–Br1	114.72(7)
2			
Zn1–N19	2.062(7)	N19–Zn1–N8 ^{iv}	109.4(3)
Zn1–N8 ^{iv}	2.072(6)	N19–Zn1–N1 ^v	100.5(3)
Zn1–N1 ^v	2.176(7)	N8–Zn1–N1 ^v	91.3(3)
Zn1–N12	2.273(7)	N19–Zn1–N12	96.0(3)
Zn1–O1	1.922(5)	N1 ^v –Zn1–N12	162.7(3)
Zn2–O1	1.968(5)	N18–Zn2–N6 ^{viii}	126.7(3)
Zn2–N18	2.082(6)	N6 ^{viii} –Zn2–N4 ^{vi}	89.3(3)
Zn2–N6 ^{viii}	2.091(7)	N18–Zn2–N15	93.3(3)
Zn2–N4 ^{vi}	2.180(7)	N6 ^{viii} –Zn2–N15	88.4(3)
Zn2–N15	2.197(7)	N4 ^{vi} –Zn2–N15	173.4(3)

Symmetry code: (i) $-x, 2-y, 2-z$; (ii) $x, 1.5-y, 0.5+z$; (iv) $x+1, y-1, z$; (v) $3-x, 1-y, -z$; (vi) $x-1, y+1, z$; (viii) $x, y-1, z$.

Preparation: All reagents were obtained commercially and used as received without further purification. The initial benzotriazol-1-yl-acetonitrile ligand was synthesized as follows: to a solution of benzotriazole (4.8 g, 40 mmol) in acetone (40 mL), K_2CO_3 (5.0 g, 36 mmol) was added into it and the mixture was stirred. A solution of bromoacetonitrile (10.8 g, 90 mmol) in acetone (15 mL) was dropped slowly into the mixture. After stirring at room temperature for 5 h, the mixture was filtered. A filtrate was evaporated to dryness under reduced pressure. The solid residue obtained was flash-chromatographed on silica

Table 3. Non-classic hydrogen bonds / $^{\circ}$ of **1** and **2**.

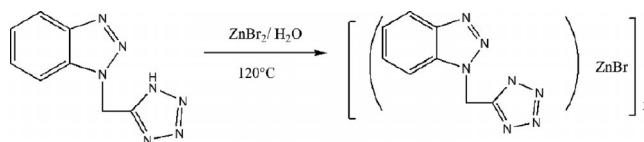
D–H \cdots A	H \cdots A	D \cdots A	DHA
1			
C8–H8A \cdots Br1 ⁱⁱⁱ	2.74	3.658(3)	159.2
C5–H5A \cdots N3 ^{viii}	2.57	3.325(4)	138.3
2			
O1–H1A \cdots N2 ^v	2.51	2.957(8)	107.9
O1–H1A \cdots N2 ^{vi}	2.39	2.963(8)	117.1
O1W–H1WA \cdots N11 ^{ix}	2.58	2.954(17)	103.6
C22–H22B \cdots N20 ^{vi}	2.57	3.373(10)	139.7
C20–H20B \cdots O1W	2.53	3.384(18)	146.6
C20–H20A \cdots N5 ^{viii}	2.53	3.298(11)	136.3
C19–H19A \cdots N3 ^x	2.48	3.358(10)	156.6
C15–H15A \cdots N12	2.62	3.449(11)	149.5
C13–H13A \cdots N5	2.55	3.158(10)	123.0
C2–H2A \cdots N7 ^{xi}	2.61	3.028(9)	106.4
a) C14–H14A \cdots Cg1		3.499(0)	160.00(5)
a) Cg2 \cdots Cg3		3.826(1)	
a) Cg3 \cdots Cg4		3.940(1)	
a) C20–H20B \cdots Cg5		3.303(1)	106.53(6)

Symmetry code: (iii) $x, 1.5-y, z-0.5$; (v) $3-x, 1-y, -z$; (vi) $x-1, y+1, z$; (viii) $x, y-1, z$; (ix) $2-x, 1-y, 1-z$; (x) $2-x, 1-y, -z$; (xi) $1+x, -2+y, z$.

a) Cg1, Cg2, Cg3, Cg4 and Cg5 are the centroid of the tetrazole or benzotriazole ring.

gel (eluent: light petroleum-acetic ester 6:1) affording the target product benzotriazol-1-yl-acetonitrile (3.74 g, 78 %, m.p. 360 K) in the last order.

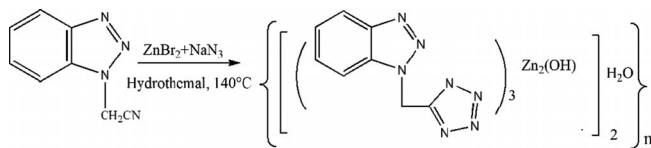
Preparation of Compound 1: Direct tetrazole-synthesis method with two-steps was used. That is to get H-1-mbtz as the first step, which was synthesized by adding benzotriazol-1-yl-acetonitrile (3.48 g, 22 mmol), sodium azide (1.43 g, 22 mmol), ZnBr_2 (4.51 g, 20 mmol), and water (40 mL) into a three-necked 250 mL round bottomed flask. The product was obtained by refluxing the reaction mixture for 24 h. After the mixture was cooled to room temperature, the pH was adjusted to 1.0 with concentrated HCl (3 M, 12 mL) to form a precipitate, which was filtered, washed with $2 \times 10 \text{ mL}$ of HCl (3 M) and dried at $80 \text{ }^{\circ}\text{C}$ overnight to get H-1-mbtz as a light yellow solid (3.08 g) in 70 % yield. The terminal product **1** was prepared under hydrothermal conditions: H-1-mbtz (4.0 mmol) and ZnBr_2 (2.0 mmol) were placed in a thick Pyrex tube (ca. 20 cm in length). After addition of water (3 mL), the tube was frozen with liquid nitrogen, evacuated, and sealed with a torch. The tube was heated at $120 \text{ }^{\circ}\text{C}$ for 4 d and finally slowly cooled to room temperature (Scheme 2). Colorless prism crystals (pure phase) suitable for X-ray analysis were formed after two weeks in 60 % yield based on ZnBr_2 . $\text{C}_8\text{H}_6\text{BrN}_7\text{Zn}$: calcd. C 27.81, H 1.75, N 28.38 %; found C 27.62, H 1.64, N 28.29 %. IR (KBr): $\tilde{\nu} = 3128 \text{ (s)}$, 3030 (s) , 2953 (s) , 1640 (s) , 1560 (s) , 1476 (m) , 1453 (m) , 1350 (m) , 1050 (s) , 789 (vs) , 705 (s) cm^{-1} .



Scheme 2.

Preparation of Compound 2: Compound **2** was prepared under hydrothermal conditions. Benzotriazol-1-yl-acetonitrile (2.0 mmol) with ZnBr_2 (1.5 mmol) in the presence of NaN_3 (3.5 mmol) were placed in a thick Pyrex tube (ca. 20 cm in length). After addition of water

(3 mL), the tube was frozen with liquid nitrogen, evacuated, and sealed with a torch. The tube was heated at 120 °C for 4 d, and after slowly cooling to room temperature (Scheme 3), colorless prism crystals (pure phase) suitable for X-ray analysis were formed after two weeks in 65% yield based on $\text{ZnBr}_2 \cdot \text{C}_{48}\text{H}_{40}\text{N}_{42}\text{O}_3\text{Zn}_4$: calcd. C 38.06, H 2.66, N 38.84%; found C 37.91, H 2.54, N 38.72%. IR (KBr): $\nu = 3416$ (w), 3050 (s), 2925 (s), 1640 (s), 1555 (s), 1483 (m), 1455 (m), 1343 (m), 1155 (m), 789 (vs), 705 (s) cm^{-1} .



Scheme 3.

Crystallographic data (excluding structure factors) for the structures in this paper have been deposited with the Cambridge Crystallographic Data Centre, CCDC, 12 Union Road, Cambridge CB21EZ, UK. Copies of the data can be obtained free of charge on quoting the depository numbers CCDC-932742 and CCDC-932743. (Fax: +44-1223-336-033; E-Mail: deposit@ccdc.cam.ac.uk, http://www.ccdc.cam.ac.uk)

Supporting Information (see footnote on the first page of this article): Details of the powder XRD pattern of **1** and **2** (Figures S1 and S2), Fluorescence spectrum of **1** in the solid state at room temperature (Figure S3).

Acknowledgements

This work was supported by the National Natural Science Foundation of China (grant No. 91022003) and the Outstanding Young Teachers of Southeast University Research Fund.

References

- J. L. C. Rowsell, A. R. Millward, K. S. Park, O. M. Yaghi, *J. Am. Chem. Soc.* **2004**, *126*, 5666.
- H. K. Chae, D. Y. Siberio-Perez, J. Kim, Y. B. Go, M. Eddaoudi, A. J. Matzger, M. O. Keeffe, O. M. Yaghi, *Nature* **2004**, *427*, 523.
- Y. Aoyama, *Top. Curr. Chem.* **1998**, *198*, 131.
- D. M. Bassani, V. Darcos, S. Mahony, J. P. Desvergne, *J. Am. Chem. Soc.* **2000**, *122*, 8795.
- M. Muthuraman, R. Masse, J. F. Nicold, G. R. Desiraju, *Chem. Mater.* **2001**, *13*, 1473.
- J. S. Miller, *Inorg. Chem.* **2000**, *39*, 4392.
- C. D. Wu, A. Hu, L. Zhang, W. B. Lin, *J. Am. Chem. Soc.* **2005**, *127*, 8940.
- J. Yang, Q. Yuo, G. D. Li, J. J. Cao, G. H. Li, J. S. Chen, *Inorg. Chem.* **2006**, *45*, 2857.
- J. L. C. Rowsell, O. M. Yaghi, *J. Am. Chem. Soc.* **2006**, *128*, 1304.
- B. L. Chen, N. W. Ockwig, A. R. Millward, D. S. Contreras, O. M. Yaghi, *Angew. Chem. Int. Ed.* **2005**, *44*, 4745.
- M. Eddaoudi, D. B. Moler, H. L. Li, B. L. Chen, T. M. Reineke, M. O'Keeffe, O. M. Yaghi, *Acc. Chem. Res.* **2001**, *34*, 319.
- Y. F. Zeng, X. Hu, F. C. Liu, X. H. Bu, *Chem. Soc. Rev.* **2009**, *38*, 469.
- X. S. Wang, Y. Z. Tang, X. F. Huang, Z. R. Qu, C. M. Che, P. W. H. Chan, R. G. Xiong, *Inorg. Chem.* **2005**, *44*, 5278.
- Q. Ye, X. S. Wang, H. Zhao, R. G. Xiong, *Chem. Soc. Rev.* **2005**, *34*, 208.
- L. Pan, N. Ching, X. Y. Huang, J. Li, *Inorg. Chem.* **2001**, *40*, 1271.
- M. T. Caudle, J. W. Kampf, M. L. Kirk, P. G. Rasmussen, V. L. Pecoraro, *J. Am. Chem. Soc.* **1997**, *119*, 9297.
- C. F. Wang, E. Q. Gao, Z. He, C. H. Yan, *Chem. Commun.* **2004**, *7*, 720.
- Y. L. Wang, D. Q. Yuan, W. H. Bi, X. Li, X. J. Li, F. Li, R. Cao, *Cryst. Growth Des.* **2005**, *5*, 1849.
- A. Panagiotis, W. K. Jeff, L. P. Vincent, *Inorg. Chem.* **2005**, *44*, 3626.
- F. Nouar, J. F. Eubank, T. Bousquet, L. Wojtas, M. J. Zaworotko, M. Eddaoudi, *J. Am. Chem. Soc.* **2008**, *130*, 1833.
- K. Nomiya, R. Noguchi, M. Oda, *Inorg. Chim. Acta* **2000**, *298*, 24.
- A. F. Stassen, M. Grunert, A. M. Mills, A. L. Spek, J. G. Haasnoot, J. Reedijk, W. Linert, *Dalton Trans.* **2003**, 3628.
- D. Fiedlere, D. H. Leung, R. G. Bergman, K. N. Raymond, *Acc. Chem. Res.* **2005**, *38*, 351.
- P. Lin, W. Clegg, R. W. Harrington, R. A. Henderson, *Dalton Trans.* **2005**, 2388.
- R. Q. Zou, L. Jiang, H. Senoh, N. Takeichi, Q. Xu, *Chem. Commun.* **2005**, 3526.
- X. W. Wang, J. Z. Chen, J. H. Liu, *Cryst. Growth Des.* **2007**, *7*, 1227.
- T. Hang, D. W. Fu, Q. Ye, H. Y. Ye, R. G. Xiong, S. D. Huang, *Cryst. Growth Des.* **2009**, *9*, 2054.
- Q. Ye, Y. M. Song, G. X. Wang, K. Chen, D. W. Fu, P. W. H. Chan, J. S. Zhu, S. D. Huang, R. G. Xiong, *J. Am. Chem. Soc.* **2006**, *128*, 6554.
- W. Wang, D. W. Fu, X. B. Xu, Q. Ye, *Z. Anorg. Allg. Chem.* **2011**, *637*, 467.
- a) Z. P. Demko, K. B. Sharpless, *J. Org. Chem.* **2001**, *66*, 7945; b) Z. P. Demko, K. B. Sharpless, *Angew. Chem. Int. Ed.* **2002**, *41*, 2113; c) Z. P. Demko, K. B. Sharpless, *Org. Lett.* **2001**, *3*, 4091; d) Z. P. Demko, K. B. Sharpless, *Angew. Chem. Int. Ed.* **2002**, *41*, 2110.
- F. Himo, Z. P. Demko, L. Noodleman, K. B. Sharpless, *J. Am. Chem. Soc.* **2003**, *125*, 9983.
- R. G. Xiong, X. Z. You, B. F. Abrahams, Z. Xue, C. M. Che, *Angew. Chem. Int. Ed.* **2001**, *40*, 4422.
- R. G. Xiong, J. Zhang, Z. F. Chen, X. Z. You, C. M. Che, H. K. Fun, *J. Chem. Soc. Dalton Trans.* **2001**, 780.
- X. Xue, X. S. Wang, L. Z. Wang, R. G. Xiong, B. F. Abrahams, X. Z. You, Z. L. Xue, C. M. Che, *Inorg. Chem.* **2002**, *41*, 6544.
- H. Zhao, Z. R. Qu, H. Y. Ye, R. G. Xiong, *Chem. Soc. Rev.* **2008**, *37*, 84.
- Y. B. Ding, Y. Cheng, Z. L. Zhang, J. Zhang, Y. G. Yin, W. H. Gao, *Inorg. Chem. Commun.* **2009**, *12*, 45.
- X. M. Zhang, *Coord. Chem. Rev.* **2005**, *249*, 1201.
- R. G. Xiong, X. Xue, H. Zhao, X. Z. You, B. F. Abrahams, Z. L. Xue, *Angew. Chem. Int. Ed.* **2002**, *41*, 3800.
- A. T. Balaban, *From Chemical Topology to Three-dimensional Geometry*, Plenum Press, New York, **1997**.
- V. A. Blatov, *IUCr Compcomm. Newslett.* **2006**, *7*, 4.
- a) G. M. Sheldrick, *SHELXS-97*, Program for Crystal Structure Solution, University of Göttingen, Germany, **1997**; b) G. M. Sheldrick, *SHELXL-97*, Program for Crystal Structure Refinement, University of Göttingen, Germany, **1997**.
- Y. Z. Tang, Y. H. Tan, D. L. Liu, X. P. Luo, X. B. Xie, Z. X. Liu, Z. T. Ge, *Inorg. Chim. Acta* **2009**, *362*, 1969.

Received: April 16, 2013
 Published Online: July 2, 2013